1521-009X/41/5/1163–1169$25.00
Drug Metabolism and Disposition

http://dx.doi.org/10.1124/dmd.113.051326
Drug Metab Dispos 41:1163–1169, May 2013

Pulmonary Metabolism of Resveratrol: In Vitro and In Vivo Evidence

Satish Sharan and Swati Nagar

Department of Pharmaceutical Sciences, Temple University School of Pharmacy, Philadelphia, Pennsylvania

Received January 30, 2013; accepted March 8, 2013

ABSTRACT

The role of pulmonary metabolism in *trans*-resveratrol (RES) pharmacokinetics was studied in a mouse model. Plasma concentrations of RES and its major metabolites *trans*-resveratrol-3-sulfate (R3S) and *trans*-resveratrol-3-glucuronide (R3G) were compared after administration of RES by intravenous (IV) and intra-arterial (IA) routes. Total area under the curve (AUC) of RES decreased by approximately 50% when RES was administered by the IV route compared with the IA route. The AUC of R3G was also significantly higher in mice administered RES by the IV route compared with the IA route. In vitro studies performed with mouse and human lung fractions confirmed pulmonary metabolism of RES. Interestingly, mouse-lung fractions gave rise to both R3S and R3G, whereas human lung fractions yielded R3S. This indicates marked interspecies variation in RES conjugation, especially in the context of extrapolating rodent data to humans. Taken together, the results presented here underline, for the first time, the impact of pulmonary metabolism on resveratrol pharmacokinetics and interspecies differences in RES pulmonary metabolism.

Introduction

The knowledge of extrahepatic metabolism in drug disposition is important. Extrahepatic drug metabolism can modify the systemic as well as tissue exposure of drug/metabolites, and this becomes especially important in cases of active metabolite formation and certain disease states. For example, in severe cirrhosis of the liver, extrahepatic metabolic pathways might compensate for the impaired hepatic elimination of a drug (Patwardhan et al., 1981). Tissue levels of drug/active metabolites might change, depending on the site of metabolism. For example, in the case of irinotecan, its active metabolite SN-38 (7-ethyl-10-hydroxy camptothecin) is conjugated to SN-38 glucuronide in the liver, which is eliminated in the bile and metabolized by gut β-glucuronidase to regenerate SN-38. Locally formed SN-38 is thought to cause diarrhea (Araki et al., 1993; Takasuna et al., 1996; Michael et al., 2004). Thus, information about sites of metabolism is important for appropriately selecting a dosage regimen for various clinical conditions, as well as for selection of appropriate route of drug administration.

The route of drug administration can significantly change the disposition of parent drug and metabolites if extrahepatic eliminating organs are involved. Although a bioavailability of 100% is assumed on intravenous (IV) administration of a drug, pulmonary metabolism can decrease the bioavailability even on IV administration. Compounds administered orally must cross the gut and lungs in addition to the liver before reaching the arterial blood supply for distribution to tissues. The lung as a site of metabolism assumes significance as the entire cardiac output (approximately four times liver blood flow) perfuses the lung and can play an important role in drug disposition (Davies and Morris, 1993). It has been shown that phenolic compounds (e.g., harmol) (Mulder et al., 1984) and phenol (Cassidy and Houston, 1984) undergo pulmonary metabolism.

Trans-resveratrol (RES) is a dietary phytochemical known to have beneficial health effects via numerous mechanisms (Baur and Sinclair, 2006). RES induces apoptosis in human lung adenocarcinoma cells (Alex et al., 2010; Zhang et al., 2011; Zhang et al., 2012b). It also has lung cancer chemopreventive activity by altering the expression of genes involved in the phase 1 metabolism of polycyclic hydrocarbons (Mollerup et al., 2001). Although the role of the gut and liver is well known in the metabolism of RES (Kuhnle et al., 2000; Miksits et al., 2005; Brill et al., 2006; Iwuchukwu and Nagar, 2008; van de Wetering et al., 2009), the role of lungs has not been evaluated in the metabolism of RES. RES is known to be extensively metabolized into its two major metabolites [i.e., *trans*-resveratrol-3-sulfate (R3S) and *trans*-resveratrol-3-glucuronide (R3G)] (Fig. 1) in humans as well as in rodents (Yu et al., 2002; Meng et al., 2004; Hoshino et al., 2010; Sharan et al., 2012). A monosulfated metabolite of RES, R3S was recently shown to be biologically active in in vitro studies (Hoshino et al., 2010). Although glucuronides have generally been assumed to be pharmacologically inactive, examples do exist of active glucuronidated metabolites (Osborne et al., 1988; Kroemer and Klotz,

This work was partially supported by awards from the National Institutes of Health (NIH) National Cancer Institute (NCI) [Grants R03CA133943 and R03CA159389]. The content is solely the responsibility of the authors and does not necessarily represent the official views of the NIH or NCI.

This work has been submitted as part of Satish Sharan's Ph.D. thesis to Temple University.

dx.doi.org/10.1124/dmd.113.051326.

ABBREVIATIONS: APAP, acetaminophen; AUC, area under the curve; BCRP (uppercase), human breast cancer resistance protein; bcrp (lowercase), mouse protein; CL, clearance; HP-β-CD, 2-hydroxypropyl-β-cyclodextrin; IA, intra-arterial; IS, internal standard; IV, intravenous; LC-MS/MS, liquid chromatography with tandem mass spectrometry; MRP (uppercase), human multidrug resistance protein; mrp (lowercase), mouse protein; PAPS, 3′-phospho-adenosine-5′-phosphosulphate; QC, quality control; RES, *trans*-3,5,4′-trihydroxystilbene, *trans*-resveratrol; R3G, *trans*-resveratrol-3-O-glucuronide; R4′G, *trans*-resveratrol-4′-O-glucuronide; R3S, *trans*-resveratrol-3-sulfate; R4′S, *trans*-resveratrol-4′-sulfate; SN-38, 7-ethyl-10-hydroxy-camptothecin; SULT, sulfotransferase; SULT (uppercase), human protein; sult (lowercase), mouse protein; UGT, uridine 5′-diphosphoglucuronosyltransferase; UGT (uppercase), human protein; ugt (lowercase), mouse protein; UDPGA, uridine 5′-diphosphoglucuronic acid; Vss, volume of distribution at steady state.

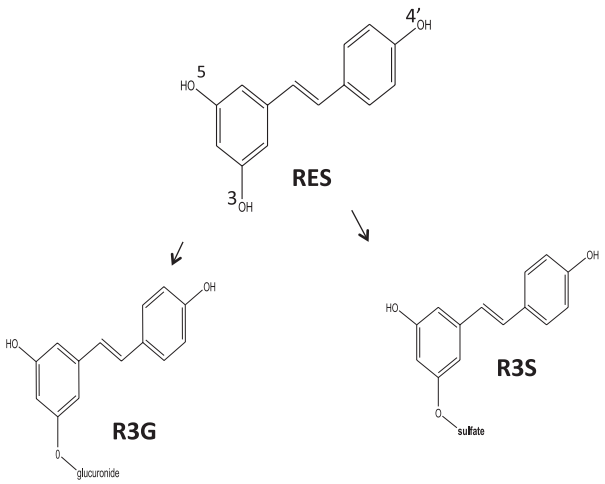

Fig. 1. Structure of RES and its major monoconjugated metabolites R3S and R3G.

1992; Sperker et al., 1997). No biologic activity of R3G has been reported to date.

In our previous study with intra-arterial (IA) administration of RES (Sharan et al., 2012), we observed that murine systemic clearance of RES was higher than hepatic blood flow, indicating the possibility of extrahepatic conjugation in the mouse. These results led us to investigate the lung as a possible metabolizing organ for RES. We studied the contribution of the pulmonary metabolism of RES in vivo by using multiple sites of administration and a single site of sampling (Cassidy and Houston, 1980), which exploits the anatomic arrangement of lungs. When administered intravenously, RES enters the right atrium of the heart and crosses the lungs in a relatively undiluted form before reaching the general arterial system for distribution throughout the body. In contrast, with IA administration into the right carotid artery, RES is available immediately for tissue distribution. By comparison of plasma concentration time profiles after administration of RES by both routes, we calculated the contribution of lungs in the first-pass metabolism of RES across the lungs. In vivo findings in mice were further confirmed by in vitro experiments using lung fractions of mouse. Finally, in vitro studies using human lung fractions were also performed to compare mouse with human RES pulmonary conjugation.

Materials and Methods

Chemicals. RES was purchased from Cayman Chemicals (Ann Arbor, MI). R3S and R3G for calibration were purchased from Toronto Research Chemicals (North York, ON, Canada).The cofactors UDPGA and PAPS (3′-phosphoadenosine-5′-phosphosulfate) were purchased from Sigma-Aldrich (St. Louis, MO). Mouse and human lung fractions were purchased from XenoTech, LLC (Lenexa, KS). Other reagents were purchased from standard sources. All reagents for analytical procedures were of analytical grade.

Animals. Male C57BL/6 mice weighing between 20 and 25 g were supplied by Jackson Laboratory and maintained in the American Association for the Accreditation of Laboratory Animal Care–accredited University Laboratory Animal Resources of Temple University. Animals were fed a normal diet, and water was continuously available. Animals were housed in a standard 12-hour dark/light cycle and were acclimatized for 4 days before the procedure. Animals had free access to food and water during the procedure. All animal studies were approved by the Institutional Animal Care and Use Committee.

Catheterization. Right carotid artery and jugular vein cannulations were performed with the animals under anesthesia with EZ-ANESTHESIA apparatus with 1.5% isoflurane and 2 l/min oxygen. An incision was made right of midline in the neck, and the right carotid artery was isolated. The right carotid artery was ligated, a small cut was made, and a medical-grade vinyl catheter tubing (0.28-mm inside diameter × 0.64 mm outside diameter, SCI, Lake Havasu City, AZ) with heparin-saline (50 IU/ml, APP Pharmaceuticals, LLC, Schaumburg, IL) was inserted with the cannula tip in the right carotid artery. The cannula was tied into place and exteriorized at the back of the neck, and the incision was sutured. The right jugular vein was cannulated in a similar manner. The cannulas were tied in place and exteriorized at the back of the neck, and the incision was sutured. Animals were allowed to recover from the surgery. Animals regained full consciousness and started moving freely 15 minutes after surgery.

Drug Administration and Blood Sampling. RES was solubilized in 20% 2-hydroxypropyl-β-cyclodextrin (HP-β-CD) in saline (Juan et al., 2010b). RES was administered by the IV route at a dose of 15 mg/kg. Carotid artery cannula was used for blood sampling. Heparin-saline (20 μl, 50 IU/ml) was used to flush the cannula after systemic administration or blood sampling. Blood (20 μl) was serially sampled at 2.5, 5, 10, 15, 45, 90, 180, 300, 420, and 600 minutes. Blood samples were centrifuged at 14,000 rpm for 2 minutes, and harvested plasma was collected and stored at −80°C until LC-MS/MS (liquid chromatography - tandem mass spectrometry) analysis. Experiment details of RES IA administration at dose of 15 mg/kg have been previously published (Sharan et al., 2012).

In Vitro Pulmonary Glucuronidation. RES glucuronidation was determined in pooled mouse lung S9 fraction and in pooled human lung microsomes. For mouse lung S9 glucuronidation assay, conditions of protein and time linearity were optimized in preliminary studies. Preliminary experiments showed that the reactions were linear up to 60 minutes and 2.5 mg/ml protein. The incubation mixture consisted of mouse lung S9 fraction (final concentration, 0.5 mg/ml), substrate RES (concentration ranging from 0.01 μM to 5 mM) solubilized in HP-β-CD (final HP-β-CD concentration 2%), alamethicin (final concentration 10 μg/ml), $MgCl_2$ (final concentration 5 mM), and made up to final incubation volume of 500 μl with Tris-HCl buffer (100 mM, pH 7.4, 37°C). The reaction mixture was preincubated for 3 minutes in a shaking water bath at 37°C. The reaction was started by adding an appropriate volume of the cofactor UDPGA (uridine 5′-diphosphoglucuronic acid, final concentration 5 mM). To 20 μl of reaction mixture, 5 μl of ascorbic acid, and 60 μl of ice-cold methanol containing acetaminophen (APAP) as internal standard (IS) were added at the end of 60 minutes to stop the reaction. All reactions were performed in triplicate. Appropriate negative control experiments were performed under the same conditions but without UDPGA.

For the human lung glucuronidation assay, incubation was performed at 0.1, 0.5, and 2.5 mg/ml (final concentration) human lung microsomes with substrate RES (0.5 mM) solubilized in HP-β-CD (final HP-β-CD concentration 2%). Preliminary studies showed minimal glucuronidation in human lung microsomes; hence kinetic assays were not conducted.

In Vitro Pulmonary Sulfation. RES sulfation activity was determined in pooled mouse lung S9 fractions and in pooled human lung S9 fractions. Conditions of protein and time linearity were optimized in preliminary studies. Preliminary experiments showed that the reactions were linear up to 60 minutes and 2.5 mg/ml total protein for each protein source. The incubation mixture consisted of mouse lung S9 fractions (final concentration, 1 mg/ml) or human lung S9 fractions (final concentration, 0.5 mg/ml), the substrate RES (0.01 μM to 5 mM) solubilized in HP-β-CD (final HP-β-CD concentration 2%), $MgCl_2$ (5 mM final concentration), and made up to final incubation volume of 500 μl with potassium phosphate buffer (10 mM, pH 6.5, 37°C). The reaction mixture was preincubated for 3 minutes in a shaking water bath at 37°C. The reaction was started by an adding appropriate volume of the cofactor PAPS (final concentration, 1 mM) and incubated in a shaking water bath for 60 minutes at 37°C. To 20 μl of reaction mixture, 5 μl of ascorbic acid and 60 μl of ice-cold methanol containing acetaminophen (APAP; internal standard, or IS) were added at the end of 60 minutes to stop the reaction. All reactions were performed in triplicate. Appropriate negative control experiments were performed under the same conditions but without PAPS.

Protein Binding Assay. Equilibrium dialysis was performed using a 96-well equilibrium dialyzer with MW cutoff of 5K (Harvard Apparatus, Holliston, MA) and placed in dual-plate rotator set to maximum speed (Harvard Apparatus) placed in a 37°C incubator with 10% CO_2 atmospheric environment. Frozen mouse plasma was thawed, and its pH was adjusted to 7.4. RES, R3S, and R3G plasma protein binding was determined at a concentration of 20 μM. The protein binding assay was performed with a published protocol (Kochansky et al., 2008).

LC-MS/MS Analysis. RES, R3S, and R3G concentrations in plasma and in the in vitro reaction mixture were measured with an electrospray ionization liquid chromatography-tandem mass spectrometry system (ABSciex API 4000; Framingham, MA) set in negative ion scan mode as described previously (Iwuchukwu et al., 2012). In brief, ascorbic acid (2.5 μl of a 15% solution) was added to 10-μl plasma samples and vortexed for 1 minute. Then 30 μl of methanol containing 78 ng/ml APAP (internal standard) was added and vortexed for 1 minute and centrifuged at 15,000 rpm for 15 minutes at room temperature. For in vitro studies, samples were prepared as described earlier herein. Supernatant (10 μl) was injected into the liquid chromatography tandem mass spectrometry system. The chromatographic separation system consisted of a guard column (Zorbax SB-C18, 5 μm, 4.6 × 12.5 mm; Agilent Technologies, Santa Clara, CA), an analytical column (Zorbax SB-C18, 5 μm, 4.6 × 150 mm; Agilent Technologies) and a gradient mobile phase of A 5 mM ammonium acetate and B methanol. The elution started with 90% A at 0 minutes to 80% at 2 minutes, 65% at 10 minutes, 40% at 12 to 17 minutes, and 90% at 19 minutes. Flow rate of the mobile phase was 1 ml/min, and the flow from the column was split 1:3 into an ABSciex API4000 triple quadrupole mass spectrometer equipped with a Turbo Ionspray source operating at 450°C. The column temperature was maintained at 35°C. The column effluent was monitored at the following precursor-product ion transitions: m/z 227→185 for RES, m/z 150→107 for IS (APAP), 403→113 for R3G, and 307→227 for R3S with a dwell time of 400 ms for each ion transition. The retention time was about 5 minutes for IS (APAP), about 5.9 minutes for R3G, about 9.2 minutes for R3S, and about 14.2 minutes for RES. The lower limit of quantification was 2.4 ng/ml for R3S and 10 ng/ml for R3G and RES.

Noncompartmental Pharmacokinetic Analysis. Pharmacokinetic parameters of RES, R3G, and R3S were analyzed by noncompartmental analysis with Phoenix, WinNonlin (version 6.1, Pharsight Corporation, Palo Alto, CA). The area under the plasma concentration-time curve (AUC) was calculated with the linear trapezoidal method; clearance (CL) was calculated as CL = dose/$AUC_{0\text{-inf}}$; volume of distribution at steady state (Vss) was calculated as Vss = CL × $MRT_{0\text{-inf}}$; the terminal half-life ($t_{1/2}$) was calculated as 0.693/λ, where λ is the slope of the terminal regression line, $AUC_{0\text{-inf}}$ is the AUC from time zero to infinity, and $MRT_{0\text{-inf}}$ is the mean residence time from time zero to infinity. The bioavailability (f_L) of RES after IV and IA administration was calculated by using eq. 1 as follows (Cassidy and Houston, 1980):

$$f_L = \left(\left[\text{mean } AUC_{0\text{-inf, i.v.}}\right]/\left[\text{mean } AUC_{0\text{-inf, i.a.}}\right]\right) \times 100. \quad (1)$$

Data Analysis for Enzyme Kinetics. All data were initially transformed, and Eadie-Hofstee (E-H) curves were plotted before nonlinear regression analysis. The Michaelis-Menten model was fit only to data that showed linear E-H plots. The following equation (eq. 2) was used to fit the data showing linear E-H plots, and Michaelis-Menten parameter estimates were determined (Segel, 1993):

$$v = Vmax*[S]/(Km + [S]), \quad (2)$$

where v is the rate of the reaction, Vmax is the maximum velocity estimate, [S] is the substrate concentration, and Km is the Michaelis-Menten constant.

The following equation (eq. 3) was used to fit the data exhibiting partial substrate inhibition profile (Hutzler and Tracy, 2002; Tracy and Hummel, 2004):

$$v = Vmax*[S]/\left(Km + [S] + \left(\frac{[S]^2}{Ki}\right)\right), \quad (3)$$

where Ki is the partial substrate inhibition constant. Nonlinear regression was performed with GraphPad Prism for Windows (version 4.03; GraphPad Software Inc., San Diego, CA).

Statistics. Student's unpaired t test was used, with $P < 0.05$ set as the significance level. GraphPad Prism for Windows (version 4.03; GraphPad Software Inc.) was used to perform statistical analysis.

Results

Noncompartmental Pharmacokinetic Analysis of RES. The concentration-time profile of RES and its metabolites after administration of RES via the IV route is shown in Fig. 2. RES (15 mg/kg).

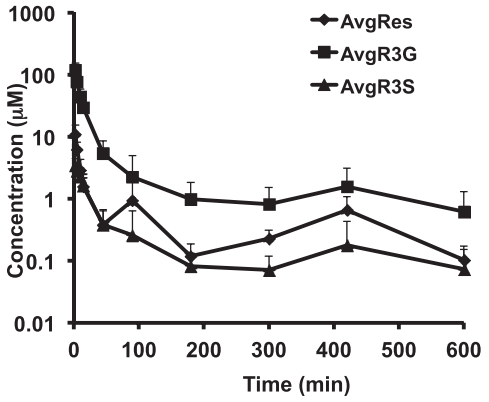

Fig. 2. Mean plasma concentration-time profile after administration of IV RES, 15 mg/kg. Data are represented as mean + S.D. (n = 5).

The IA data were previously published (Sharan et al., 2012). Both IV and IA experiments were conducted in parallel under the same laboratory conditions; therefore, we were able to compare the data. RES was metabolized into two major metabolites: R3S and R3G. The results of the noncompartmental pharmacokinetic analysis are summarized in Table 1.

RES exposure (294.98 ± 137.87 minutes*μM) and half-life (101.30 ± 43.41 minutes) after IV administration were significantly lower than its exposure (591.08 ± 167.29 minutes*μM) and half-life (190.58 ± 69.65 minutes) after IA administration (AUC: $P = 0.01$, $t_{1/2}$: $P = 0.04$). The bioavailability (f_L) of RES after IV administration was 49.9%. The clearance and volume of distribution at steady state of RES after IV administration were not statistically significantly different compared with those after IA administration (CL: $P = 0.05$, Vss: $P = 0.85$). Interestingly, it was observed that the exposure of R3G (2268.35 ± 517.00 minutes*μM) after IV administration of RES increased significantly compared with R3G exposure (921.23 ± 457.07 minutes*μM) after RES IA administration ($P = 0.004$). No significant change was observed in the exposure of R3S after RES administration by both routes ($P = 0.67$).

The plasma protein binding of RES, R3G, and R3S in mouse plasma was found to be 91.95 ± 0.99, 66.75 ± 1.56, and 87.24 ± 4.89% (mean ± SD, n = 3) respectively.

In Vitro Pulmonary Metabolism. The glucuronidation of RES was studied in mouse and human lung fractions. Figure 3A shows the formation rate of R3G in mouse lung fraction with its Eadie-Hofstee

TABLE 1

Noncompartmental pharmacokinetic analysis on a single intra-arterial (IA) dose, 15 mg/kg. RES dose and an intravenous (IV) RES dose, 15 mg/kg RES dose

Data are presented as estimate ± S.D.

RES	RES 15 mg/kg IA[a] (n = 5)	RES 15 mg/kg IV (n = 5)	Units
AUC0-inf	591.08 ± 167.29[b]	294.98 ± 137.87[b]	min*μM
Cl	118.77 ± 33.36	280.04 ± 158.25	ml/min/kg
Vss	37.59 ± 23.70	34.90 ± 20.10	l/kg
$t_{1/2}$	190.58 ± 69.65[b]	101.30 ± 43.41[b]	min
R3G			
AUC0-inf	921.23 ± 457.07[b]	2268.35 ± 517.00[b]	min*μM
R3S			
AUC0-inf	174.94 ± 45.75	157.21 ± 77.77	min*μM

AUC, area under the curve; Cl, clearance; R3G, *trans*-resveratrol-3-O-glucuronide; RES, *trans*-3,5,4'-trihydroxystilbene (*trans*-resveretrol); $t_{1/2}$, half-time; Vss, volume of distribution at steady state.

[a]Data are from (Sharan et al., 2012).

[b]Denotes statistically significant parameters between the IA versus IV groups, with an unpaired student t test, and $P < 0.05$ considered significant.

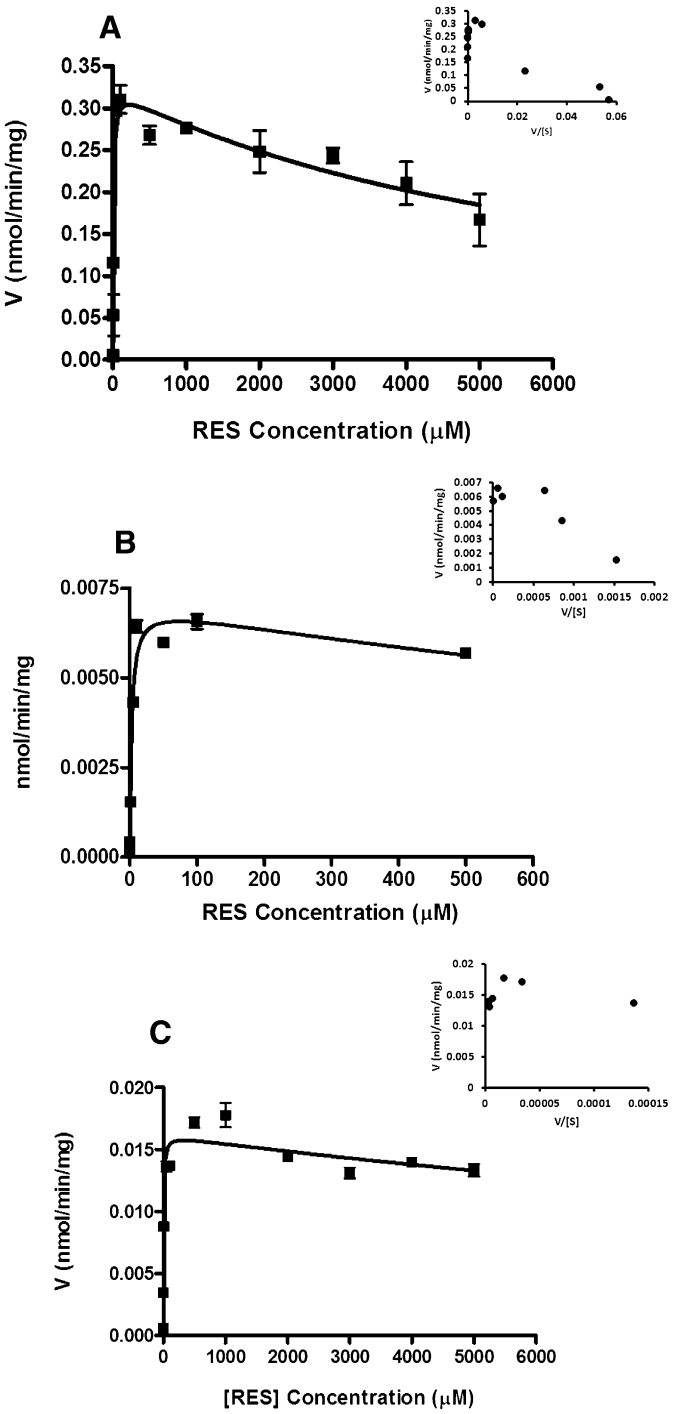

Fig. 3. In vitro kinetics of (A) R3G formation in mouse lung S9 fraction, (B) R3S formation in mouse lung S9 fraction, and (C) R3S formation in human lung S9 fraction. Data are reported as mean ± S.D. (n = 3). The solid line represents curve fitting with the partial substrate inhibition equation (eq. 3); the inset represents Eadie-Hofstee plots.

(E-H) plot shown as inset. The R3G profile exhibited partial substrate inhibition. This was determined by fitting the data to the partial substrate inhibition equation

The E-H plot showed a hook in the upper quadrant typical of partial substrate inhibition kinetic profile (Fig. 3A inset; eq. 3) (Hutzler and Tracy, 2002). Enzyme kinetic parameters are presented in Table 2. When RES was incubated with 0.1 and 0.5 mg/ml human lung microsomes, no R3G was observed above LOQ (limit of quantitation, 10 ng/ml for R3G) at the end of 60 minutes' incubation. Therefore, no further RES glucuronidation kinetic studies were performed with human lung microsomes.

Fig. 3, B and C show the formation kinetics of R3S in mouse and human lung fractions with E-H plots as insets respectively. R3S formation in both mouse and human lung fractions showed partial substrate inhibition (Hutzler and Tracy, 2002).

Discussion

RES is known to be extensively metabolized into its conjugates, mainly R3G and R3S (Yu et al., 2002; Meng et al., 2004; Hoshino et al., 2010; Iwuchukwu et al., 2012). Lungs are the third in a series of three potential biotransformation sites (along with the gut and liver) that orally ingested RES must cross before entering the general circulation. First-pass metabolism by gut, liver, and lungs in series can synergistically increase total body clearance of RES. Although the role of gut and liver in the metabolism of RES is known (Miksits et al., 2005; Brill et al., 2006; Iwuchukwu and Nagar, 2008), the contribution of lungs to RES metabolism has not been evaluated. In the present study, the contribution of lungs in the metabolism of RES was evaluated using multiple sites of administration and a single site of sampling design (Cassidy and Houston, 1980) in a mouse model. The in vivo study clearly demonstrated the contribution of lungs in the glucuronidation of RES to R3G in mice. In vivo results were corroborated by in vitro studies in mouse lung fractions.

Because species-dependent differences in metabolism are known, in vitro studies were also conducted in human lung fractions to determine whether reliable extrapolation of data can be made between mice and humans. Interestingly, no significant glucuronidation of RES was observed in human lung fractions, implying that the contribution of pulmonary glucuronidation in the metabolism of RES might be quantitatively less important in humans. The species difference in RES glucuronidation at its 3-OH position can be explained by differential expression of urindine 5′-diphosphoglucuronosyltransferase (UGT) isoforms in mouse and human lungs. RES has been reported to be glucuronidated at its 3-OH position via UGT1A1, UGT1A7, and UGT1A9, with minor contribution from UGT1A6, UGT1A8, UGT1A10, and UGT2B7 (Brill et al., 2006). Ugt1a6 has been shown to be expressed well in mouse lung (Buckley and Klaassen, 2007) and might be responsible for RES glucuronidation in mouse lungs. There are conflicting reports about the presence of UGT enzymes in human lung. UGT1A1 and UGT1A10 have been reported in lung cancer samples (Oguri et al., 2004). Several UGT2B isozymes are reportedly present in human lungs (Turgeon et al., 2001). UGT expression and activity have been reported in the upper respiratory tract but not in lungs in humans (Zheng et al., 2002), which becomes important for inhaled compounds. Other studies have shown low or no UGT expression in normal human lung tissue (Zheng et al., 2002; Somers et al., 2007; Nakamura et al., 2008). In the present study, the absence of R3G formation in human lung fraction is consistent with low or absent expression of UGT isoforms in normal human lung tissue (Nakamura et al., 2008) responsible for RES glucuronidation (Brill et al., 2006).

Sulfation experiments showed that RES is sulfated by both mouse and human lungs. RES sulfation at its 3-OH position has been reported via sulfotransferase (SULT) 1A1, SULT1A2, SULT1A3, and SULT1E1 isoforms (Miksits et al., 2005). Mouse lungs express sult1a1, with very low expression of sult1e1 (Alnouti and Klaassen, 2006). SULT1A1, SULT1A3, SULT1E1, SULT2A1, and SULT1B1 are expressed in human lungs, and SULT1A1, SULT1A3, and

TABLE 2

Kinetic parameter estimates for the sulfation and glucuronidation of RES and R3S by human and mouse lung fractions

Data are expressed as estimates ± SD; n = 3. Estimate units are as follows: Vmax: nanomoles per minute per milligram total protein; Km, Ki: micromolar.

Substrate	Conjugation Product	Protein Source	Vmax (pmol/min/mg)	Km (μM)	Ki (μM)	Goodness of Fit (r^2)	Type of Fit
RES	R3G	Mouse lung S9	324.40 ± 13.05	7.34 ± 1.60	6632 ± 1198	0.93	Partial substrate inhibition
RES	R3S	Mouse lung S9	7.05 ± 0.28	2.69 ± 0.45	2021 ± 717.6	0.96	Partial substrate inhibition
RES	R3S	Human lung S9	16.15 ± 0.48	4.45 ± 0.79	23,238 ± 7305	0.95	Partial substrate inhibition

Ki, partial substrate inhibition constant; Km, the Michaelis-Menten constant; R3G, *trans*-resveratrol-3-O-glucuronide; R3S, *trans*-resveratrol-3-sulfate; RES, *trans*-3,5,4'-trihydroxystilbene (*trans*-resveratrol).

SULT1E1 account for around 80% of all SULTs expressed in human lungs (Riches et al., 2009). Therefore, sult1a1 and sult1e1 in mouse lungs and SULT1A1, SULT1A3, and SULT1E1 in human lungs might be responsible for R3S formation. Steroid sulfatase activity has been reported in both human (Milewich et al., 1983) and mouse lung tissue (Milewich et al., 1984), with the highest activity in microsomal fractions of human lung tissue homogenates (Milewich et al., 1983). Steroid sulfatase can desulfate R3S to give RES locally in the lung cells. This futile cycling of RES/R3S by the combined activity of sulfatase and sulfotransferase enzyme can lead to an increase in the retention of the RES/R3S within the lung. This can be important since RES and R3S both have been shown to have pharmacological activity in vitro (Hoshino et al., 2010).

Transporters, in conjunction with metabolizing enzymes, play an important role in the disposition of drugs and metabolites. R3G and R3S disposition is known to be influenced by transporters. R3G has been shown to be a high affinity substrate for human multidrug resistance protein transporter (MRP) 2 (ABCC2), MRP3 (ABCC3), and human breast cancer resistance protein (BCRP; ABCG2) transporters (Maier-Salamon et al., 2008; van de Wetering et al., 2009; Juan et al., 2010a). Although the role of MRP1 (ABCC1) specifically in R3G transport has not been evaluated, there are reports of MRP1-mediated transport of glucuronides such as 17β-estradiol-glucuronide (Jedlitschky et al., 1996), etoposide glucuronides, SN-38 glucuronide (Deeley and Cole, 2006), and β-O-glucuronide conjugate of the tobacco-specific carcinogen 4-(methylnitrosamino)-1-(3-pyridyl)-1-butanol (NNAL) (Leslie et al., 2001). BCRP and MRP2 are involved in the transport of R3S (van de Wetering et al., 2009; Juan et al., 2010a). MRP4 (ABCC4) and MRP1 (ABCC1) have not been studied for R3S transport, but both MRP4 and MRP1 are reportedly involved in the transport of sulfo-conjugates such as dehydroepiandrosterone sulfate (Zelcer et al., 2003) and estrone 3-sulfate (Qian et al., 2001). Mouse lungs have been shown to express Mrp1, Mrp3, and Mrp4 transporters (Maher et al., 2005). It is interesting that mouse lungs did not express Mrp2 and Bcrp transporter (Scheffer et al., 2002; Maher et al., 2005).

Cellular distribution and localization of transporters in mouse lungs are unknown, although cellular distribution and localization of MRP1, MRP2, and BCRP in human lungs are reported. MRP1 is expressed on the basolateral membrane, whereas MRP2 and BCRP are expressed toward the apical membrane in human lungs (Bosquillon, 2010). Although cellular localization of MRP3 and MRP4 transporters is unknown in lungs, they are expressed on the basolateral side in hepatocytes (Zamek-Gliszczynski et al., 2006).

Based on present results and previous reports (Maher et al., 2005; Bosquillon, 2010), a simplified scheme for the disposition of RES, R3S, and R3G in mouse lung cells is proposed (Fig. 4A). RES, administered by the IV route, can diffuse into mouse lung cells and can either get metabolized by sult enzymes present in the cytosol or ugt enzymes present in the endoplasmic reticulum. Additionally, R3S formed from RES can get further desulfated by sulfatase enzymes in the endoplasmic reticulum to give RES, which can further get glucuronidated to R3G. This R3G can diffuse into the cytoplasm and be transported into the blood by Mrp3 and possibly Mrp1. This correlates well with our observation that even after sulfation of RES in lungs (based on our in vitro results), we did not observe any significant difference in the plasma exposure of R3S when RES was administered by the IV route compared with the IA route. Similarly, a schematic pathway for disposition of RES in human lungs has been proposed (Fig. 4B). RES, when presented to human lung cells, gets sulfated to R3S in the cytoplasm. R3S formed can be eliminated in the pulmonary lumen by MRP2 and BCRP or into blood by MRP1 and MRP4. Additionally, it can be desulfated by steroid sulfatase in the endoplasmic reticulum to give back RES. Since no activity of UGT was observed in human lung tissue, RES formed in endoplasmic reticulum can act as a depot, or it can diffuse back into cytoplasm to again get sulfated to R3S. This futile cycling of RES/R3S can prolong the presence of RES/R3S in human lung tissue.

The pulmonary metabolism of RES can have implications for local tissue levels, as well as systemic concentrations of parent and metabolites. The absence of pulmonary glucuronidation in human lung compared with extensive pulmonary glucuronidation in mouse lungs is a possible reason for the observed difference in the pharmacokinetics of RES in rodents versus humans. In rodents, R3G has been observed as the quantitatively major metabolite (Juan et al., 2010b; Colom et al., 2011; Iwuchukwu et al., 2012; Sharan et al., 2012) compared with R3S in humans (Boocock et al., 2007; Brown et al., 2010).

Our results might have implications in the role of RES as a cancer chemopreventive in the lung. As a substrate for SULTs, RES might interfere with the metabolism of cigarette-smoke toxicants. For example, sulfation of benzo[a]pyrene-7,8-catechol has been suggested to be a detoxification pathway for benzo[a]pyrene-7,8-dione by limiting its ability to undergo redox cycling (Zhang et al., 2012a). Also, increased RES or R3S in the lung can lead to enhanced quenching of unstable free radicals and can lead to reduced DNA damage by reactive oxygen species, which are known to be produced by cigarette-smoke toxicants. Interestingly, RES and R3S have been shown to have comparable ability to quench the 2,2-diphenyl-1-picrylhydrazyl (DPPH) free radical (Hoshino et al., 2010).

In summary, significantly higher R3G exposure was observed in mouse when RES was administered by the IV route compared with the IA route. Extensive glucuronidation and sulfation of RES were observed in mouse lung fractions. Human lung fractions on the other hand showed only sulfation of RES and a potential for futile cycling of RES/R3S in lung, which can have pharmacological significance. In conclusion, pulmonary metabolism of RES might play an important role in the pharmacokinetics and activity of RES.

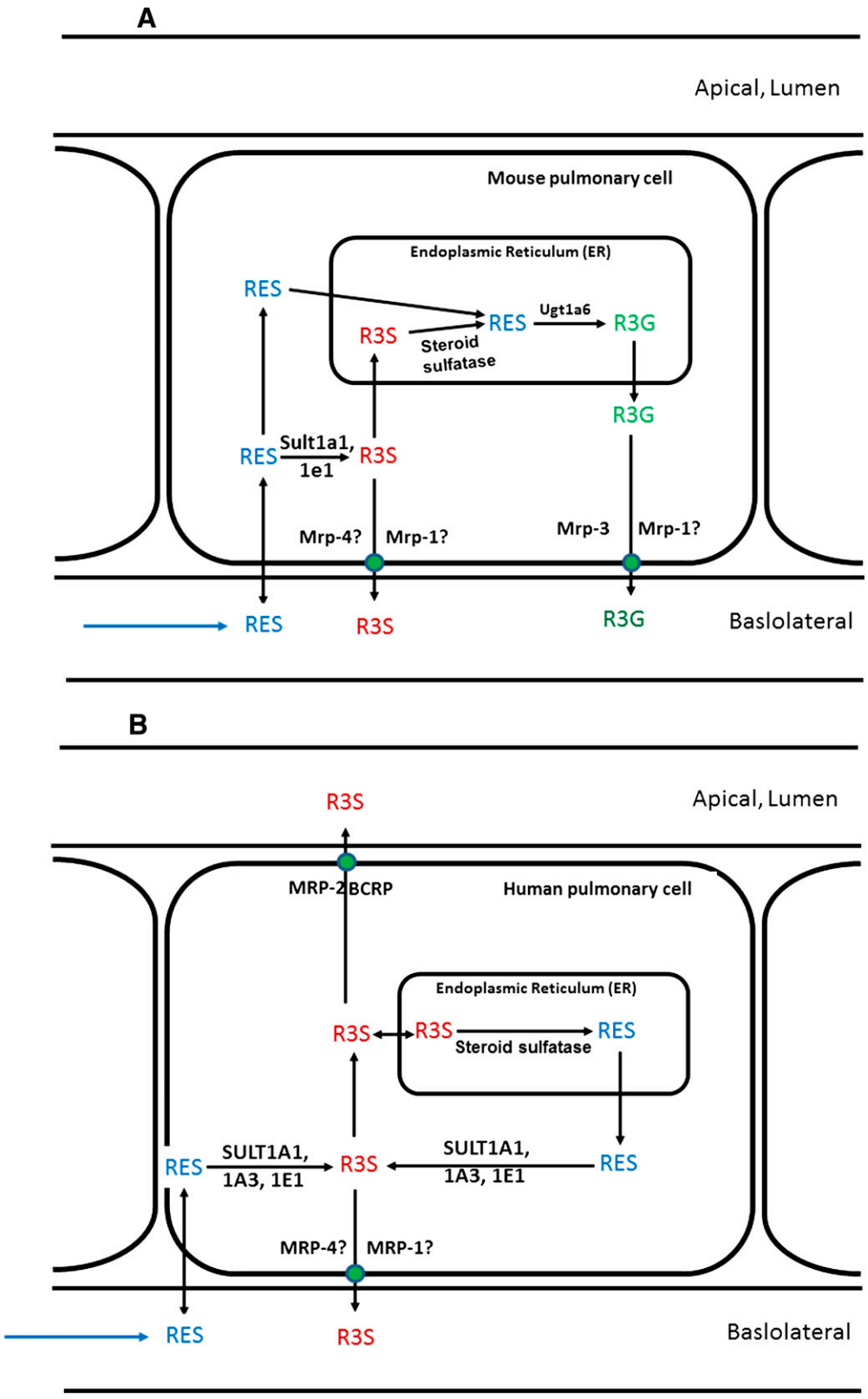

Fig. 4. Proposed schematic representation of RES metabolism in (A) mouse lung cells and (B) human lung cells. Solid arrows represent pathways based on results in this manuscript and published literature reports for metabolism and/or transport of RES, R3S, and R3G. Transporters followed by "?" indicates that the role of these transporters has not been established for transport of R3S and R3G but is hypothesized based on literature detailed in the *Discussion*.

Acknowledgments

The authors thank Temple University School of Pharmacy for support and Priyanka Kulkarni for technical assistance.

Authorship Contributions

Participated in research design: Sharan, Nagar.
Conducted experiments: Sharan.
Performed data analysis: Sharan, Nagar.
Wrote or contributed to the writing of the manuscript: Sharan, Nagar.

References

Alex D, Leong EC, Zhang ZJ, Yan GT, Cheng SH, Leong CW, Li ZH, Lam KH, Chan SW, and Lee SM (2010) Resveratrol derivative, trans-3,5,4′-trimethoxystilbene, exerts anti-angiogenic and vascular-disrupting effects in zebrafish through the downregulation of VEGFR2 and cell-cycle modulation. *J Cell Biochem* **109**:339–346.

Alnouti Y and Klaassen CD (2006) Tissue distribution and ontogeny of sulfotransferase enzymes in mice. *Toxicol Sci* **93**:242–255.

Araki E, Ishikawa M, Iigo M, Koide T, Itabashi M, and Hoshi A (1993) Relationship between development of diarrhea and the concentration of SN-38, an active metabolite of CPT-11, in the intestine and the blood plasma of athymic mice following intraperitoneal administration of CPT-11. *Jpn J Cancer Res* **84**:697–702.

Baur JA and Sinclair DA (2006) Therapeutic potential of resveratrol: the in vivo evidence. *Nat Rev Drug Discov* **5**:493–506.

Boocock DJ, Faust GE, Patel KR, Schinas AM, Brown VA, Ducharme MP, Booth TD, Crowell JA, Perloff M, and Gescher AJ, et al. (2007) Phase I dose escalation pharmacokinetic study in healthy volunteers of resveratrol, a potential cancer chemopreventive agent. *Cancer Epidemiol Biomarkers Prev* **16**:1246–1252.

Bosquillon C (2010) Drug transporters in the lung: do they play a role in the biopharmaceutics of inhaled drugs? *J Pharm Sci* **99**:2240–2255.

Brill SS, Furimsky AM, Ho MN, Furniss MJ, Li Y, Green AG, Bradford WW, Green CE, Kapetanovic IM, and Iyer LV (2006) Glucuronidation of trans-resveratrol by human liver and intestinal microsomes and UGT isoforms. *J Pharm Pharmacol* **58**:469–479.

Brown VA, Patel KR, Viskaduraki M, Crowell JA, Perloff M, Booth TD, Vasilinin G, Sen A, Schinas AM, and Piccirilli G, et al. (2010) Repeat dose study of the cancer chemopreventive agent resveratrol in healthy volunteers: safety, pharmacokinetics, and effect on the insulin-like growth factor axis. *Cancer Res* **70**:9003–9011.

Buckley DB and Klaassen CD (2007) Tissue- and gender-specific mRNA expression of UDP-glucuronosyltransferases (UGTs) in mice. *Drug Metab Dispos* **35**:121–127.

Cassidy MK and Houston JB (1980) In vivo assessment of extrahepatic conjugative metabolism in first pass effects using the model compound phenol. *J Pharm Pharmacol* **32**:57–59.

Cassidy MK and Houston JB (1984) In vivo capacity of hepatic and extrahepatic enzymes to conjugate phenol. *Drug Metab Dispos* **12**:619–624.

Colom H, Alfaras I, Maijó M, Juan ME, and Planas JM (2011) Population pharmacokinetic modeling of trans-resveratrol and its glucuronide and sulfate conjugates after oral and intravenous administration in rats. *Pharm Res* **28**:1606–1621.

Davies B and Morris T (1993) Physiological parameters in laboratory animals and humans. *Pharm Res* **10**:1093–1095.

Deeley RG and Cole SP (2006) Substrate recognition and transport by multidrug resistance protein 1 (ABCC1). *FEBS Lett* **580**:1103–1111.

Hoshino J, Park EJ, Kondratyuk TP, Marler L, Pezzuto JM, van Breemen RB, Mo S, Li Y, and Cushman M (2010) Selective synthesis and biological evaluation of sulfate-conjugated resveratrol metabolites. *J Med Chem* **53**:5033–5043.

Hutzler JM and Tracy TS (2002) Atypical kinetic profiles in drug metabolism reactions. *Drug Metab Dispos* **30**:355–362.

Iwuchukwu OF and Nagar S (2008) Resveratrol (trans-resveratrol, 3,5,4′-trihydroxy-trans-stilbene) glucuronidation exhibits atypical enzyme kinetics in various protein sources. *Drug Metab Dispos* **36**:322–330.

Iwuchukwu OF, Sharan S, Canney DJ, and Nagar S (2012) Analytical method development for synthesized conjugated metabolites of trans-resveratrol, and application to pharmacokinetic studies. *J Pharm Biomed Anal* **63**:1–8.

Jedlitschky G, Leier I, Buchholz U, Barnouin K, Kurz G, and Keppler D (1996) Transport of glutathione, glucuronate, and sulfate conjugates by the MRP gene-encoded conjugate export pump. *Cancer Res* **56**:988–994.

Juan ME, González-Pons E, and Planas JM (2010a) Multidrug resistance proteins restrain the intestinal absorption of trans-resveratrol in rats. *J Nutr* **140**:489–495.

Juan ME, Maijó M, and Planas JM (2010b) Quantification of trans-resveratrol and its metabolites in rat plasma and tissues by HPLC. *J Pharm Biomed Anal* **51**:391–398.

Kochansky CJ, McMasters DR, Lu P, Koeplinger KA, Kerr HH, Shou M, and Korzekwa KR (2008) Impact of pH on plasma protein binding in equilibrium dialysis. *Mol Pharm* **5**:438–448.

Kroemer HK and Klotz U (1992) Glucuronidation of drugs: a re-evaluation of the pharmacological significance of the conjugates and modulating factors. *Clin Pharmacokinet* **23**:292–310.

Kuhnle G, Spencer JP, Chowrimootoo G, Schroeter H, Debnam ES, Srai SK, Rice-Evans C, and Hahn U (2000) Resveratrol is absorbed in the small intestine as resveratrol glucuronide. *Biochem Biophys Res Commun* **272**:212–217.

Leslie EM, Ito K, Upadhyaya P, Hecht SS, Deeley RG, and Cole SP (2001) Transport of the beta -O-glucuronide conjugate of the tobacco-specific carcinogen 4-(methylnitrosamino)-1-(3-pyridyl)-1-butanol (NNAL) by the multidrug resistance protein 1 (MRP1): requirement for glutathione or a non-sulfur-containing analog. *J Biol Chem* **276**:27846–27854.

Maher JM, Slitt AL, Cherrington NJ, Cheng X, and Klaassen CD (2005) Tissue distribution and hepatic and renal ontogeny of the multidrug resistance-associated protein (Mrp) family in mice. *Drug Metab Dispos* **33**:947–955.

Maier-Salamon A, Hagenauer B, Reznicek G, Szekeres T, Thalhammer T, and Jäger W (2008) Metabolism and disposition of resveratrol in the isolated perfused rat liver: role of Mrp2 in the biliary excretion of glucuronides. *J Pharm Sci* **97**:1615–1628.

Meng X, Maliakal P, Lu H, Lee MJ, and Yang CS (2004) Urinary and plasma levels of resveratrol and quercetin in humans, mice, and rats after ingestion of pure compounds and grape juice. *J Agric Food Chem* **52**:935–942.

Michael M, Brittain M, Nagai J, Feld R, Hedley D, Oza A, Siu L, and Moore MJ (2004) Phase II study of activated charcoal to prevent irinotecan-induced diarrhea. *J Clin Oncol* **22**:4410–4417.

Miksits M, Maier-Salamon A, Aust S, Thalhammer T, Reznicek G, Kunert O, Haslinger E, Szekeres T, and Jaeger W (2005) Sulfation of resveratrol in human liver: evidence of a major role for the sulfotransferases SULT1A1 and SULT1E1. *Xenobiotica* **35**:1101–1119.

Milewich L, Garcia RL, and Gerrity LW (1984) Steroid sulfatase and 17 beta-hydroxysteroid oxidoreductase activities in mouse tissues. *J Steroid Biochem* **21**:529–538.

Milewich L, Garcia RL, and Johnson AR (1983) Steroid sulfatase activity in human lung tissue and in endothelial pulmonary cells in culture. *J Clin Endocrinol Metab* **57**:8–14.

Mollerup S, Ovrebø S, and Haugen A (2001) Lung carcinogenesis: resveratrol modulates the expression of genes involved in the metabolism of PAH in human bronchial epithelial cells. *Int J Cancer* **92**:18–25.

Mulder GJ, Weitering JG, Scholtens E, Dawson JR, and Pang KS (1984) Extrahepatic sulfation and glucuronidation in the rat in vivo: determination of the hepatic extraction ratio of harmol and the extrahepatic contribution to harmol conjugation. *Biochem Pharmacol* **33**:3081–3087.

Nakamura A, Nakajima M, Yamanaka H, Fujiwara R, and Yokoi T (2008) Expression of UGT1A and UGT2B mRNA in human normal tissues and various cell lines. *Drug Metab Dispos* **36**:1461–1464.

Oguri T, Takahashi T, Miyazaki M, Isobe T, Kohno N, Mackenzie PI, and Fujiwara Y (2004) UGT1A10 is responsible for SN-38 glucuronidation and its expression in human lung cancers. *Anticancer Res* **24** (5A):2893–2896.

Osborne R, Joel S, Trew D, and Slevin M (1988) Analgesic activity of morphine-6-glucuronide. *Lancet* **1**:828.

Patwardhan RV, Johnson RF, Hoyumpa A, Jr, Sheehan JJ, Desmond PV, Wilkinson GR, Branch RA, and Schenker S (1981) Normal metabolism of morphine in cirrhosis. *Gastroenterology* **81**:1006–1011.

Qian YM, Song WC, Cui H, Cole SP, and Deeley RG (2001) Glutathione stimulates sulfated estrogen transport by multidrug resistance protein 1. *J Biol Chem* **276**:6404–6411.

Riches Z, Stanley EL, Bloomer JC, and Coughtrie MW (2009) Quantitative evaluation of the expression and activity of five major sulfotransferases (SULTs) in human tissues: the SULT "pie." *Drug Metab Dispos* **37**:2255–2261.

Scheffer GL, Pijnenborg AC, Smit EF, Müller M, Postma DS, Timens W, van der Valk P, de Vries EG, and Scheper RJ (2002) Multidrug resistance related molecules in human and murine lung. *J Clin Pathol* **55**:332–339.

Segel I (1993) *Enzyme Kinetics: Behavior and Analysis of Rapid Equilibrium and Steady-State Enzyme Systems*, Wiley-Interscience, New York.

Sharan S, Iwuchukwu OF, Canney DJ, Zimmerman CL, and Nagar S (2012) In vivo-formed versus preformed metabolite kinetics of trans-resveratrol-3-sulfate and trans-resveratrol-3-glucuronide. *Drug Metab Dispos* **40**:1993–2001.

Somers GI, Lindsay N, Lowdon BM, Jones AE, Freathy C, Ho S, Woodrooffe AJ, Bayliss MK, and Manchee GR (2007) A comparison of the expression and metabolizing activities of phase I and II enzymes in freshly isolated human lung parenchymal cells and cryopreserved human hepatocytes. *Drug Metab Dispos* **35**:1797–1805.

Sperker B, Backman JT, and Kroemer HK (1997) The role of beta-glucuronidase in drug disposition and drug targeting in humans. *Clin Pharmacokinet* **33**:18–31.

Takasuna K, Hagiwara T, Hirohashi M, Kato M, Nomura M, Nagai E, Yokoi T, and Kamataki T (1996) Involvement of beta-glucuronidase in intestinal microflora in the intestinal toxicity of the antitumor camptothecin derivative irinotecan hydrochloride (CPT-11) in rats. *Cancer Res* **56**:3752–3757.

Tracy TS and Hummel MA (2004) Modeling kinetic data from in vitro drug metabolism enzyme experiments. *Drug Metab Rev* **36**:231–242.

Turgeon D, Carrier JS, Lévesque E, Hum DW, and Bélanger A (2001) Relative enzymatic activity, protein stability, and tissue distribution of human steroid-metabolizing UGT2B subfamily members. *Endocrinology* **142**:778–787.

van de Wetering K, Burkon A, Feddema W, Bot A, de Jonge H, Somoza V, and Borst P (2009) Intestinal breast cancer resistance protein (BCRP)/Bcrp1 and multidrug resistance protein 3 (MRP3)/Mrp3 are involved in the pharmacokinetics of resveratrol. *Mol Pharmacol* **75**:876–885.

Yu C, Shin YG, Chow A, Li Y, Kosmeder JW, Lee YS, Hirschelman WH, Pezzuto JM, Mehta RG, and van Breemen RB (2002) Human, rat, and mouse metabolism of resveratrol. *Pharm Res* **19**:1907–1914.

Zamek-Gliszczynski MJ, Nezasa K, Tian X, Bridges AS, Lee K, Belinsky MG, Kruh GD, and Brouwer KL (2006) Evaluation of the role of multidrug resistance-associated protein (Mrp) 3 and Mrp4 in hepatic basolateral excretion of sulfate and glucuronide metabolites of acetaminophen, 4-methylumbelliferone, and harmol in Abcc3-/- and Abcc4-/- mice. *J Pharmacol Exp Ther* **319**:1485–1491.

Zelcer N, Reid G, Wielinga P, Kuil A, van der Heijden I, Schuetz JD, and Borst P (2003) Steroid and bile acid conjugates are substrates of human multidrug-resistance protein (MRP) 4 (ATP-binding cassette C4). *Biochem J* **371**:361–367.

Zhang L, Huang M, Blair IA, and Penning TM (2012a) Detoxication of benzo[a]pyrene-7,8-dione by sulfotransferases (SULTs) in human lung cells. *J Biol Chem* **287**:29909–29920.

Zhang W, Wang X, and Chen T (2011) Resveratrol induces mitochondria-mediated AIF and to a lesser extent caspase-9-dependent apoptosis in human lung adenocarcinoma ASTC-a-1 cells. *Mol Cell Biochem* **354**:29–37.

Zhang W, Wang X, and Chen T (2012b) Resveratrol induces apoptosis via a Bak-mediated intrinsic pathway in human lung adenocarcinoma cells. *Cell Signal* **24**:1037–1046.

Zheng Z, Fang JL, and Lazarus P (2002) Glucuronidation: an important mechanism for detoxification of benzo[a]pyrene metabolites in aerodigestive tract tissues. *Drug Metab Dispos* **30**:397–403.

Address correspondence to: Dr. Swati Nagar, Temple University School of Pharmacy, 3307 N Broad Street, Philadelphia PA 19140. E-mail: swati.nagar@temple.edu